

European Validation of SAGE II Aerosol Profiles

M. ACKERMAN,^{1,2} C. BROGNIEZ,³ B. S. DIALLO,³ G. FIOCCO,⁴ P. GOBBI,⁵
M. HERMAN,³ M. JÄGER,⁶ J. LENOBLE,³ C. LIPPENS,² G. MÉGIE,⁷
J. PELON,⁷ R. REITER,^{6,8} AND R. SANTER³

A SAGE II validation program has been performed in Europe using ground-based lidars and balloon-borne polarimetric and photographic experiments. Between the tropopause height and about 23 km, good agreement is found between the SAGE II 1.02- μm extinction profiles and the lidar profiles, using for the conversion of backscattering into extinction an aerosol model consistent with the SAGE II spectral extinction. The extinction profiles deduced from the limb photographs at 0.44 and 0.375 μm present a good agreement with the SAGE II profiles at 0.453 and 0.385 μm , respectively. The size distribution retrieved from the near-infrared polarimetric observations leads to a spectral variation of the extinction in good agreement with SAGE II data in the same altitude range. Above 23–25 km the observations are scarce and the data of poorer quality because of the low aerosol content. The 1.02- μm extinction profiles seem to agree with the ruby lidar and the limb photograph profiles. But any conclusion concerning the short-wavelength profiles and the size distribution at these high altitudes would be risky.

1. INTRODUCTION

SAGE II provides aerosol extinction profiles at 1.02, 0.525, 0.453, and 0.385 μm . The 1.02- μm channel is free from any other contribution except the Rayleigh correction, which is not too large for most of the altitude range. The results are retrieved without difficulties almost down to the ground level in cloud-free cases. The upper limit of retrieval is due to the low aerosol concentration, which leads to transmissions very close to 1 above some altitudes (around 30 km at middle latitudes), for the present state of the atmosphere; smoothing procedures allow retrieval at higher altitudes, but with increasing error bars. The three short-wavelength channels are contaminated by ozone and nitrogen dioxide absorption; the separation of these contributions has been discussed by *Chu et al.* [this issue]. The upper limit of a reasonable quality retrieved profile is probably a little below 30 km for the three channels, because of the increasing contribution of O_3 and NO_2 with altitude. Moreover, the Rayleigh correction increases toward the short wavelengths, leading to an increasing error in the retrieved extinctions and limiting the retrieval to altitudes above 8, 10, and 14 km for the 0.525-, 0.453-, and 0.385- μm aerosol extinction profiles, respectively.

The aerosol extinction depends on their total number density and on their size distribution, as well as on their shape and refractive index; they are generally assumed to be

spherical droplets of an aqueous sulfuric acid solution. This means that there is no direct, simple validation experiment for the aerosol data as there is for the gas data, where only one parameter (the gas concentration) has to be measured. The most direct approach is to measure in situ the absolute size distribution $n(r)$ of the particles (including the total number $N = \int_0^\infty n(r) dr$ per unit volume) and to compute by Mie theory the extinction profiles to be compared to the SAGE II extinction profiles. This can be achieved by various instruments, such as wire impactors, quartz crystal microbalance (QCM) multifilters, and optical counters [*Russell et al.*, 1981, 1984; *Oberbeck et al.*, 1986; *Osborn et al.*, this issue]; however, all instruments have limitations in the range of sizes detected. Another approach consists of using other scattering measurements that should be consistent with the SAGE II extinction profiles. The best known example of this procedure is the lidar backscattering profile. The backscattering data have to be converted into extinction profiles, using a model of the aerosol size distribution and the Mie theory; for consistency, the same model must reproduce the spectral variation of the extinction deduced from the four SAGE II aerosol channels.

During the correlative experiments made in Europe [*Lenoble*, this issue], ground-based lidars were used at four different stations; the results are presented in section 2. Two other scattering techniques have been simultaneously used from balloon platforms: photographs of the Earth's limb and infrared polarimetric measurements. These are presented with some details in sections 3 and 4, respectively. Analysis and comparisons of the results are discussed in section 5.

2. LIDAR

Nd: Yag lasers operating at 0.532 μm have been used at the Observatoire de Haute Provence (OHP), Frascati, and Florence, and a ruby laser operating at 0.694 μm has been used at Garmisch-Partenkirchen. All of the lidar profiles are corrected for extinction; the three lidars are calibrated assuming $R_{\text{min}} = 1$ in the altitude range 30–40 km. The ruby laser allows retrieval of the profiles up to altitudes higher than the Nd: Yag laser, because of the smaller contribution of Rayleigh scattering at the larger wavelength. The data provided by the experimenters are the backscattering ratio

¹Authors are listed in alphabetical order.

²Institut d'Aéronomie Spatiale de Belgique, Brussels, Belgium.

³Laboratoire d'Optique Atmosphérique, Université des Sciences et Techniques de Lille, Villeneuve d'Ascq, France.

⁴Instituto di Fisica "Guglielmo Marconi", Università Degli Studi Roma, Rome, Italy.

⁵Instituto di Fisica dell'Atmosfera, Consiglio Nazionale della Ricerche, Frascati, Italy.

⁶Institut für Atmosphärische Umweltforschung, Garmisch-Partenkirchen, Federal Republic of Germany.

⁷Service d'Aéronomie du Centre National de la Recherche Scientifique, Verrières-le-Buisson, France.

⁸Now at Consulting Bureau, Garmisch-Partenkirchen, Federal Republic Germany.

Copyright 1989 by the American Geophysical Union.

Paper number 89JD00242.
0148-0227/89/89JD-00242\$05.00

$R = (b^{\text{aer}} + b^{\text{mol}})/b^{\text{mol}}$, versus the altitude; b^{aer} is the aerosol and b^{mol} the molecule backscattering coefficient.

The aerosol backscattering is deduced from R and b^{mol} (computed for a standard atmosphere). The aerosol extinction coefficient is related to the backscattering coefficient by

$$\sigma^{\text{aer}}(\lambda) = 4\pi b^{\text{aer}}(\lambda)/p^{\text{aer}}(\lambda, 180^\circ) \quad (1)$$

where $p^{\text{aer}}(\lambda, 180^\circ)$ is the aerosol phase function (normalized at 4π). The exact phase function, which depends on the characteristics and size distribution of the aerosols, is unknown. Therefore it is replaced by the phase function computed for an "aerosol model." The same model is used to transform $\sigma^{\text{aer}}(\lambda)$ into $\sigma^{\text{aer}}(1.02)$ for comparison with the SAGE II profiles at $1.02 \mu\text{m}$. The following transformation equations are used:

$$b^{\text{aer}}(\lambda) = (R - 1)b^{\text{mol}}(\lambda) \quad (2)$$

$$\sigma^{\text{aer}}(\lambda) = 4\pi b^{\text{aer}}(\lambda)/[p^{\text{aer}}(\lambda, 180^\circ)]^{\text{model}} \quad (3)$$

$$\sigma^{\text{aer}}(1.02) = \sigma^{\text{aer}}(\lambda)[\sigma^{\text{aer}}(1.02)/\sigma^{\text{aer}}(\lambda)]^{\text{model}} \quad (4)$$

or combining (2), (3), and (4),

$$\sigma^{\text{aer}}(1.02) = 4\pi(R - 1)b^{\text{mol}}(\lambda)/K(\lambda) \quad (5)$$

where

$$K(\lambda) = [\sigma^{\text{aer}}(\lambda)p^{\text{aer}}(\lambda, 180^\circ)/\sigma^{\text{aer}}(1.02)]^{\text{model}} \quad (6)$$

We have chosen to compare the lidar data with the SAGE II profiles at $1.02 \mu\text{m}$, because they are of better quality and are retrieved at higher altitudes than the SAGE II profiles at $0.525 \mu\text{m}$, which are closer to the lidar wavelengths. Similarly, the statistical error ΔR due to signal fluctuations is transformed into an error $\Delta\sigma^{\text{aer}}(1.02)$. The conversion of backscattering at λ into extinction at $1.02 \mu\text{m}$ has been made with various models, and it has proved insensitive to the detailed shape of the size distribution, the main parameter being the effective radius r_{eff} and the effective variance v_{eff} , defined by

$$r_{\text{eff}} = \int_0^\infty r^3 n(r) dr / \int_0^\infty r^2 n(r) dr \quad (7)$$

$$v_{\text{eff}} = \int_0^\infty (r - r_{\text{eff}})^2 r^2 n(r) dr / r_{\text{eff}}^2 \int_0^\infty r^2 n(r) dr \quad (8)$$

The simplest choice for modeling is a lognormal size distribution (LND):

$$n(r) = (N/\sqrt{2\pi r \ln s}) \exp\left[-\frac{\ln^2 r/r_m}{2 \ln^2 s}\right] \quad (9)$$

The r_{eff} and v_{eff} are related to the mean radius r_m and the variance s by [Lenoble and Brogniez, 1984]

$$r_{\text{eff}} = r_m \exp(2.5 \ln^2 s) \quad (10)$$

$$v_{\text{eff}} = \exp(\ln^2 s) - 1 \quad (11)$$

Figure 1 presents the conversion factor ($K(\lambda) = \sigma^{\text{aer}}(\lambda)p^{\text{aer}}(\lambda, 180^\circ)/\sigma^{\text{aer}}(1.02)$) versus r_{eff} for LND models (75% H_2SO_4 droplets at 220 K), with $v_{\text{eff}} = 0.25$ ($s = 1.60$), for the two lidars. It varies slowly for r_{eff} larger than $0.20 \mu\text{m}$ and is almost constant for r_{eff} larger than $0.30 \mu\text{m}$; but it increases

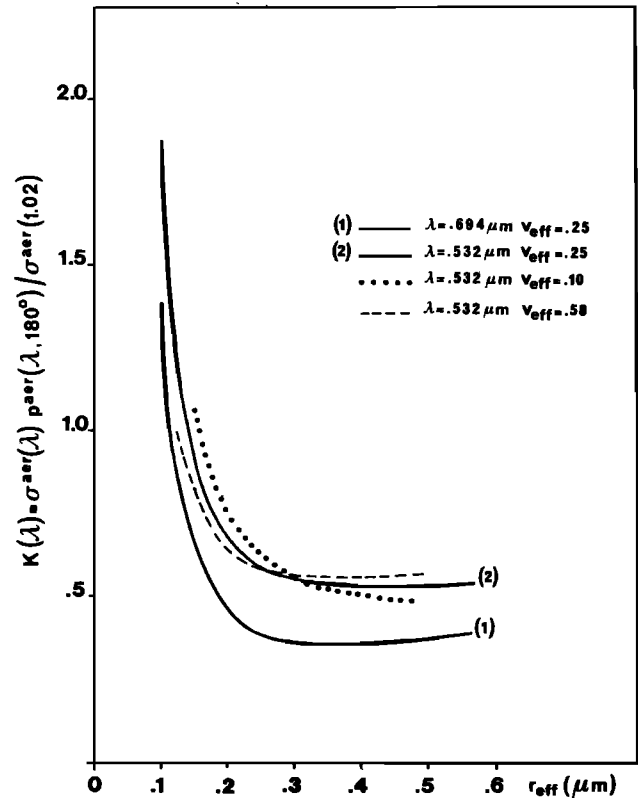


Fig. 1. Lidar conversion factor $K(\lambda)$ versus the effective radius r_{eff} for aerosol LND models; particles are 75% H_2SO_4 at 220 K.

very rapidly for smaller particles. Similar curves can be drawn for other values of v_{eff} . However, the influence of v_{eff} becomes large only for particles smaller than $0.20 \mu\text{m}$; it is almost negligible for $r_{\text{eff}} = 0.30 \mu\text{m}$, as K increases with v_{eff} for $r_{\text{eff}} > 0.30 \mu\text{m}$ and decreases for $r_{\text{eff}} < 0.30 \mu\text{m}$. For example, the curves corresponding to $v_{\text{eff}} = 0.1$ and $v_{\text{eff}} = 0.58$ at $\lambda = 0.532 \mu\text{m}$ are shown in Figure 1.

The results of the lidar/SAGE II profile comparisons will be presented, using for the conversion of backscattering into extinction the model (or models) with $v_{\text{eff}} = 0.25$, which gives the best agreement between the two profiles. The choice will be checked for consistency with the SAGE II spectral extinction and/or with the in situ observations in section 5.

The four periods of observations were November 10–13, 1984, November 27–30, 1984, April 21–23, 1985, and October 12–14, 1985; the locations of the SAGE II events and of the ground stations are presented by Lenoble [this issue].

2.1. November 10–13, 1984

During the period from November 10 through 13, 1984, the aerosol layer was very unstable on the local scale, as shown by the in situ balloon observations, and on the scale of the observation zone, as proved by the important differences between the six SAGE II profiles. The lidar profiles obtained at OHP and at Garmisch-Partenkirchen on November 11 are also quite different, as are the profiles obtained at OHP on November 11 and November 13. However, on November 13 the situation seems to stabilize and the two SAGE II profiles at 8.49°W (1703 UT) and 15.8°E (1527 UT) are very similar; this allows a comparison with the OHP lidar profile obtained at the same latitude and 6°E , from 1705 to 1817 UT (Figure

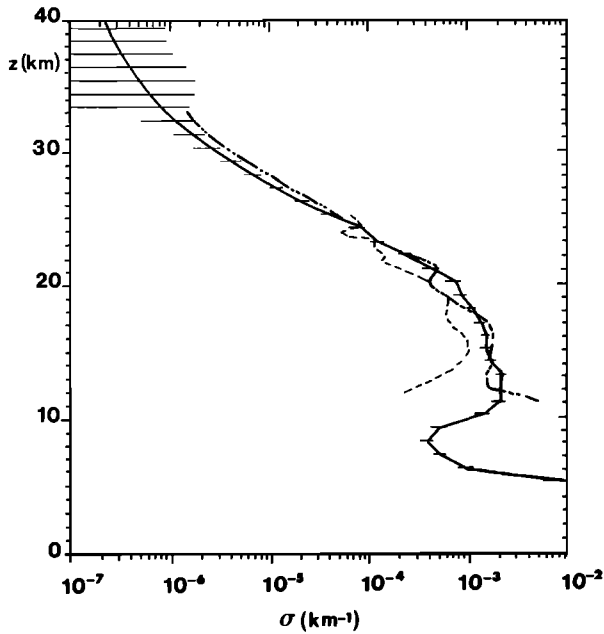


Fig. 2. Comparison of aerosol extinction profiles at $1.02 \mu\text{m}$ from SAGE II and retrieved from lidar backscattering with a LND model $r_{\text{eff}} = 0.25$ (see text) on November 13, 1984: solid curve, SAGE II, 1703 UT, 44.62°N , 8.49°W ; dash-double-dotted curve, SAGE II, 1527 UT, 44.50°N , 15.81°E (error bars omitted); dashed curve, OHP lidar, 1705–1817 UT, 44°N , 6°E (aerosol model: $r_{\text{eff}} = 0.35 \mu\text{m}$).

2). The agreement is very good above 18 km and certainly within the error limits of the lidar profile; below 18 km the differences are probably due to the variability of the aerosol layer. The conversion from backscattering into extinction has been made with a LND model, $r_{\text{eff}} = 0.35 \mu\text{m}$, for all altitudes. But as mentioned earlier, the conversion is not very sensitive to the effective radius in this size range and any model with r_{eff} between 0.20 and $0.50 \mu\text{m}$ would lead to a similar agreement.

2.2. November 26–30, 1984

For the period November 26–30, 1984, the situation was more stable. From the eight SAGE II profiles, only the western profiles of November 28 and 29 seem to correspond to a different air mass with more aerosols above 25 km; the other six profiles (eastern profiles for the whole period and western profiles for November 26 and 27) are very similar. The several lidar profiles obtained during this period (OHP, November 27–29; Frascati, November 28–30; Garmisch-Partenkirchen, November 27) confirm a good stability for the aerosol layer over the zone and the period. This provides conditions much better than during the middle of November for a comparison program. Figures 3, 4, and 5 present the results of these comparisons. For November 27 (Figure 3), two lidar profiles are available: one from OHP up to 25 km and one from Garmisch-Partenkirchen up to 30 km. To obtain agreement with SAGE II, the conversion from backscattering into extinction has to be made using models with a particle size decreasing with altitude z ; we have used $r_{\text{eff}} = 0.25 \mu\text{m}$ for $z < 21 \text{ km}$, $r_{\text{eff}} = 0.10 \mu\text{m}$ for $21 \text{ km} < z < 25 \text{ km}$, and $r_{\text{eff}} = 0.05 \mu\text{m}$ for $z > 25 \text{ km}$; a gradual change of r_{eff} with altitude is more likely than an abrupt one, but should appear around 20–22 km and 25–26 km. Above 28 km, even smaller

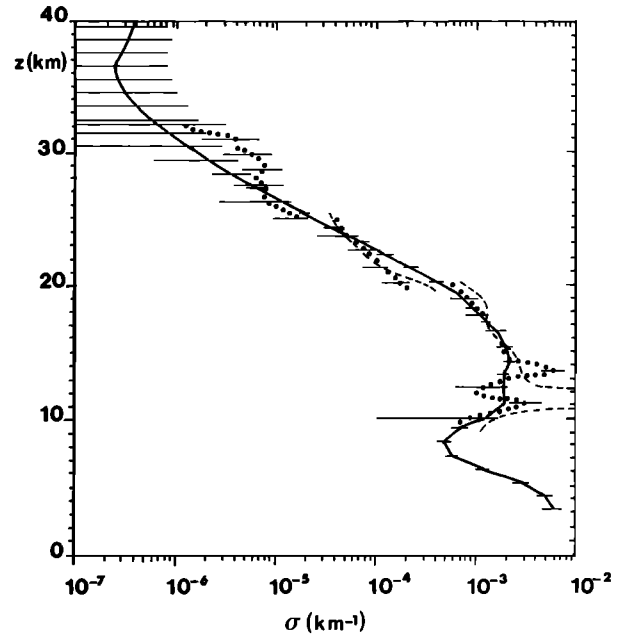


Fig. 3. Same as Figure 2 except on November 27, 1984: solid curve, SAGE II, 1457 UT, 46.53°N , 18.63°E ; dashed curve, lidar OHP, 1720 UT, 44°N , 6°E ; dotted curve, Garmisch-Partenkirchen lidar, 47.5°N , 11°E (aerosol model: $r_{\text{eff}} = 0.25 \mu\text{m}$, $z < 21 \text{ km}$; $r_{\text{eff}} = 0.10 \mu\text{m}$, $21 \text{ km} < z < 25 \text{ km}$; $r_{\text{eff}} = 0.05 \mu\text{m}$, $z > 25 \text{ km}$).

particles would give better agreement than the model with $r_{\text{eff}} = 0.05 \mu\text{m}$, but the accuracy of both the SAGE II and the lidar profiles is probably not good enough at these altitudes to give a definite conclusion. The error bars on the Garmisch-Partenkirchen lidar profile have been given every 2 km; they are somewhat larger for the OHP lidar profile.

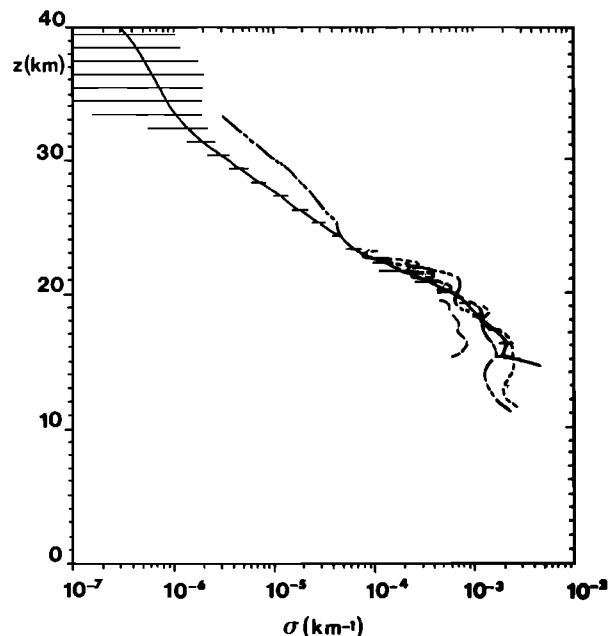


Fig. 4. Same as Figure 2, except on November 28, 1984: solid curve, SAGE II, 1509 UT, 45.18°N , 16.76°E ; dash-double-dotted curve, SAGE II, 1645 UT, 45.07°N , 7.36°W (error bars omitted); dashed curve, OHP lidar, 1657–1830 UT, 44°N , 6°E ; long-dashed curve, Frascati lidar, 1800 UT, 42°N , 13°E (aerosol model: $r_{\text{eff}} = 0.25 \mu\text{m}$).

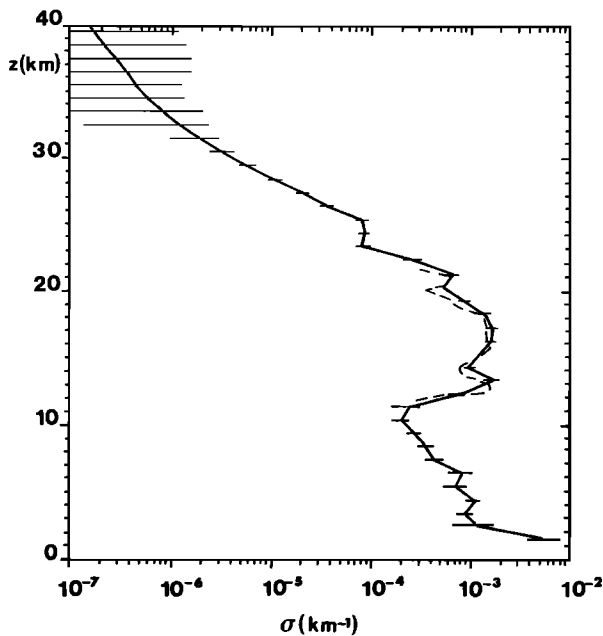


Fig. 5. Same as Figure 2, except on November 30, 1984: solid curve, SAGE II 1533 UT, 41.40°N, 13.61°E; long-dashed curve, Frascatti lidar, 1936 UT, 42°N, 13°E (aerosol model: $r_{\text{eff}} = 0.35 \mu\text{m}$).

The two lidar profiles agree with each other reasonably well, as well as with the SAGE II profile above 15 km; below this level they exhibit oscillations, probably due to local conditions. For November 28 (Figure 4) the conversion has been made with $r_{\text{eff}} = 0.25 \mu\text{m}$ up to 23 km, which is the upper limit of the lidar profiles (OHP and Frascatti). The agreement between the OHP lidar and the SAGE II profiles is very good; the Frascatti lidar leads to somewhat smaller extinctions below 20 km. November 30 (Figure 5) corresponds to the closest coincidence, as the SAGE II tangent point is about 90 km from Frascatti. The conversion has been made with $r_{\text{eff}} = 0.35 \mu\text{m}$, and the agreement between the Frascatti lidar and the SAGE II profiles is almost perfect in the altitude range of the lidar profile (12–22 km).

2.3. April 1985

In April 1985 the five SAGE II aerosol profiles available over the zone are almost identical, pointing to very stable conditions for the aerosol layer. Unfortunately, weather conditions did not permit lidar observations, except at Garmisch-Partenkirchen on April 21. As the SAGE II tangent points were not very close to Garmisch-Partenkirchen on April 21, and considering the homogeneity mentioned earlier, we have chosen to make the comparison with the average SAGE II profile for the considered zone and period. The result of this comparison is presented in Figure 6. The bars on the SAGE II average profile in Figure 6 are the standard deviations; they are of the same order as the error bars on individual profiles. No error bars have been given for the lidar profile, but the errors can be expected to be of the same order as in Figure 3. The conversion of backscattering into extinction had to be made with $r_{\text{eff}} = 0.35 \mu\text{m}$ below 21 km and $r_{\text{eff}} = 0.10 \mu\text{m}$ above that level in order to find the best agreement between the two profiles; the change of particle size seems rather abrupt between 20–22 km. The agreement is within the error bars.

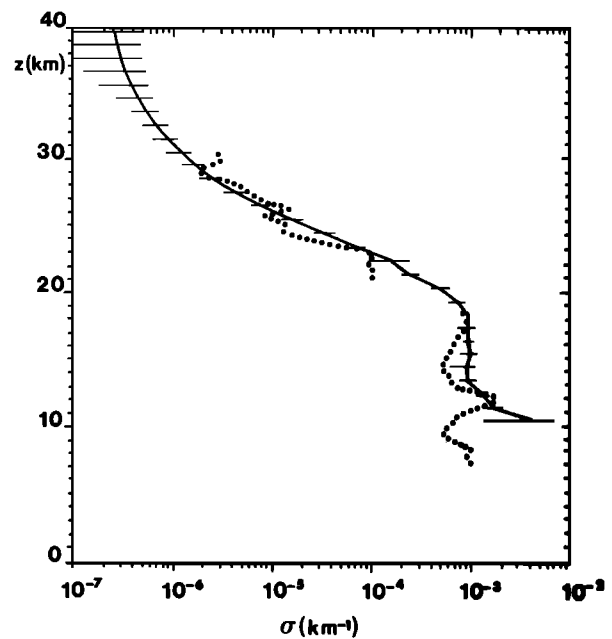


Fig. 6. Same as Figure 2, except on April 21, 1985: solid curve, SAGE II, average of five profiles (April 21–23 between 50.14° and 43.80°N and 7.20°W and 21.29°E) with standard deviations; dotted curve, Garmisch-Partenkirchen lidar, April 21, 47.5°N; 11°E (aerosol model: $r_{\text{eff}} = 0.35 \mu\text{m}$, $z < 21 \text{ km}$; $r_{\text{eff}} = 0.10 \mu\text{m}$, $z > 21 \text{ km}$).

2.4. October 1985

In October 1985 the six SAGE II profiles are rather similar, but not as similar as in April. Lidar profiles were obtained at OHP for 4 successive days, and they show a good stability of the aerosol layer at this station. Figure 7

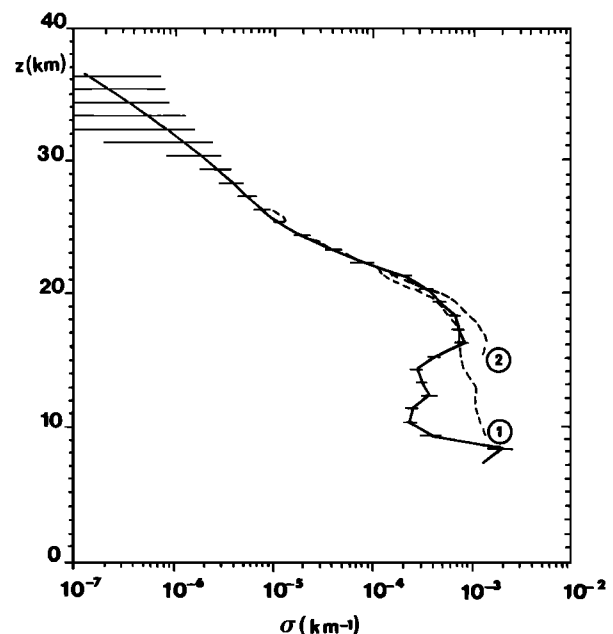


Fig. 7. Same as Figure 2, except on October 12, 1985: solid curve, SAGE II, 0502 UT, 41.03°N, 17.03°E; dashed curve, OHP lidar, 1900–1920 UT, 44°N, 6°E (1, aerosol model $r_{\text{eff}} = 0.17 \mu\text{m}$; 2, aerosol model deduced from polarization measurements).

compares the OHP lidar profile for the evening of October 12 with the SAGE II morning profile on October 12, approximately 10° east of OHP. The SAGE II profile at about 14° west of OHP is very similar above 16 km and so are the two profiles for the morning of October 13, however, with values slightly higher above 21 km for the eastern profile. Below 16 km the four profiles are quite different, and no comparison can be sought. A good agreement above 16 km is found by using an aerosol model with $r_{\text{eff}} = 0.17 \mu\text{m}$ for the conversion of the lidar profile.

In conclusion, the extinction profiles retrieved from lidar profiles seem in reasonably good agreement (generally within the error bars) with the SAGE II extinction profiles at $1.02 \mu\text{m}$, provided r_{eff} is chosen suitably. The best validation is obtained on November 30, 1984, where there is a close coincidence in time and location between the SAGE II and the Frascati lidar profiles (Figure 5). The periods of stability of the aerosol layer allow rather good validations with noncoincident observations; this is the case for April 21–24, 1985 (Figure 5). The conversion of backscattering lidar profiles into extinction profiles has to be done with variable models, the particle sizes being generally smaller at high altitudes. The consistency of the choice of the model with the other observations will be discussed in section 5.

3. BALLOON LIMB PHOTOGRAPHS

Photographs of the limb radiance were made from balloons at Aire sur l'Adour by the Institut d'Aéronomie Spatiale de Belgique (IASB); the photographs were made for low Sun elevation, at various solar azimuths for two wavelengths (0.84 and $0.44 \mu\text{m}$) during the first flight and for three wavelengths (0.84 , 0.44 , and $0.375 \mu\text{m}$) during the second flight [Ackerman *et al.*, 1981]. The extinction is deduced from the radiance measured at 30° scattering angle, and the Rayleigh extinction is subtracted to obtain the aerosol extinction. Only direct solar radiation falling on the atmosphere is considered, since the solar elevation is low and since it has been checked that the effects of illumination by clouds or lower atmospheric layers are negligible. Only single scattering is taken into account, which is reasonable, since only observations at low extinction are used. Most of the uncertainties originate from film calibration ($\pm 20\%$). A value equal to 3 is used for the phase function at 30° . The uncertainty is here equal to $\pm 15\%$ for a range of asymmetry parameters from 0.4 to 0.7. Two flights took place, on November 10, 1984, and April 22, 1985. They were simultaneous to flights of the polarimetric instrument described in section 4.

3.1. November 10, 1984

On November 10, 1984, the photographs confirm the aerosol layer inhomogeneity mentioned previously (section 2). To the south of the balloon position, well-marked vertical structures were observed [Ackerman *et al.*, 1985]. Toward the north a much smoother vertical profile was observed. The SAGE II tangent point on November 10 is rather far to the southeast, over the Mediterranean Sea, and the SAGE II profiles on November 11, closer to the balloon launch site, are completely different than the November 10 profiles. We have therefore chosen to compare the balloon profiles with the two SAGE II profiles of November 10 and 11 in Figures

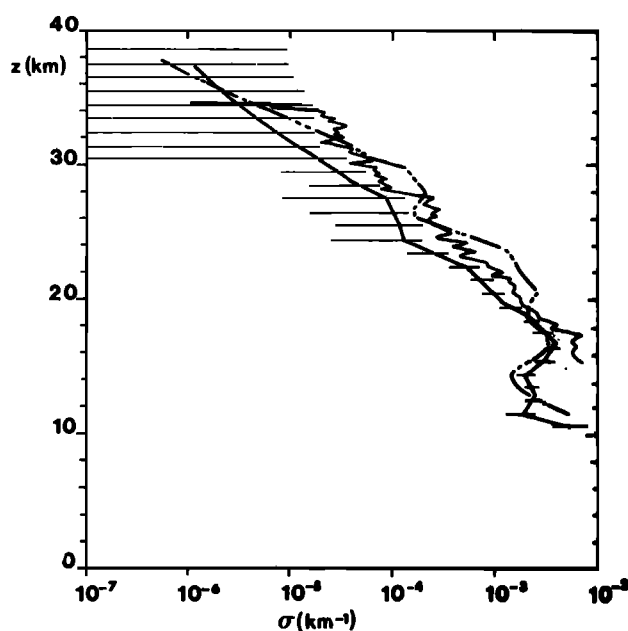


Fig. 8. Comparison of aerosol extinction profiles from SAGE II on November 10, 1984, at 1627 UT, 37.80°N , 5.27°E ; (dash-double-dotted curve) and SAGE II on November 11, 1984, at 1639 UT, 40.50°N , 0.56°E (solid curve) and from balloon limb photographs on November 10, 1984, at sunset, launch site 44°N , 0° (thin solid curve); SAGE II $\lambda = 0.453 \mu\text{m}$; balloon $\lambda = 0.44 \mu\text{m}$.

8 and 9. Figure 8 compares the balloon profile at $0.44 \mu\text{m}$ with the two SAGE II profiles at $0.453 \mu\text{m}$; we have not introduced a correction for the small wavelength difference. Figure 9 concerns the comparison at $1.02 \mu\text{m}$; the balloon profiles at $0.84 \mu\text{m}$ have been converted to $1.02 \mu\text{m}$, using two aerosol models with $r_{\text{eff}} = 0.28 \mu\text{m}$ and $r_{\text{eff}} = 0.05 \mu\text{m}$, respectively, but the conversion is not very sensitive to the model. At $1.02 \mu\text{m}$ the balloon profile on November 10 and

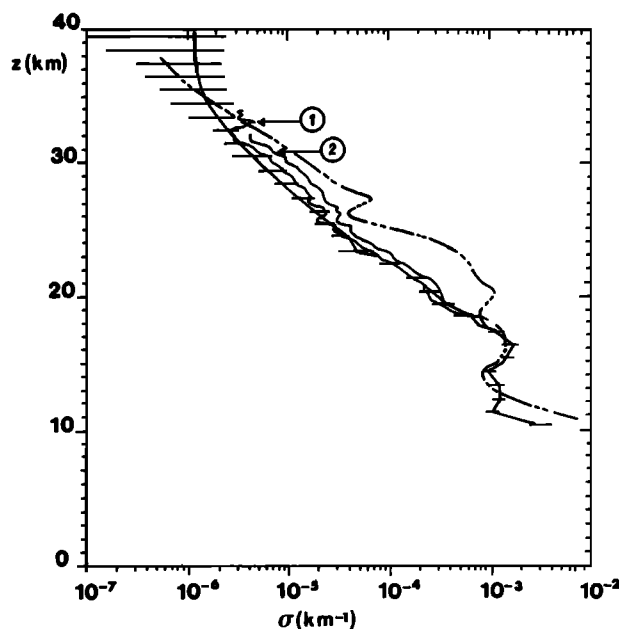


Fig. 9. Same as Figure 8, except $\lambda = 1.02 \mu\text{m}$. Balloon data are converted from 0.84 to $1.02 \mu\text{m}$ with LND aerosol models, $v_{\text{eff}} = 0.10$; 1, $r_{\text{eff}} = 0.05 \mu\text{m}$; 2, $r_{\text{eff}} = 0.28 \mu\text{m}$.

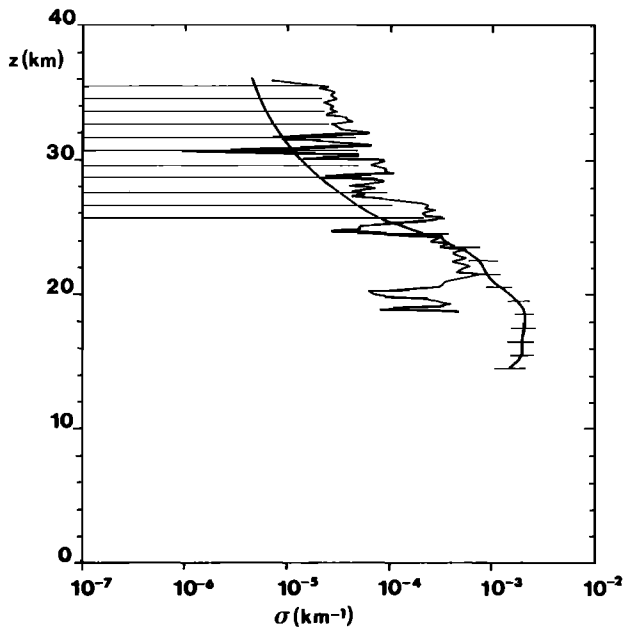


Fig. 10. Comparison of aerosol extinction profiles from SAGE II on April 22, 1985, at 1906 UT, 47.17°N, 2.90°W (solid curve) and from balloon limb photographs on April 22, 1985, at sunset, launch site 44°N, 0° (thin solid curve); SAGE II $\lambda = 0.385 \mu\text{m}$; balloon $\lambda = 0.375 \mu\text{m}$.

the SAGE II profile on November 11 are in very close agreement, whereas the SAGE II profile on November 10 is quite different. At 0.44/0.453 μm , the balloon profile is between the two SAGE II profiles, with a general shape more similar to the SAGE II profile of November 11.

3.2. April 22, 1985

On April 22, 1985, the conditions were very stable, and the air mass observed at 30° from the Sun and for a tangent

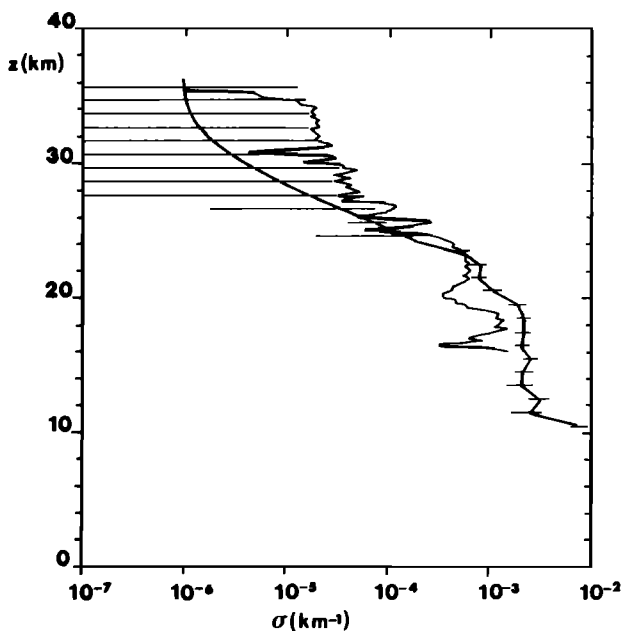


Fig. 11. Same as Figure 10, except SAGE II $\lambda = 0.453 \mu\text{m}$; balloon $\lambda = 0.44 \mu\text{m}$.

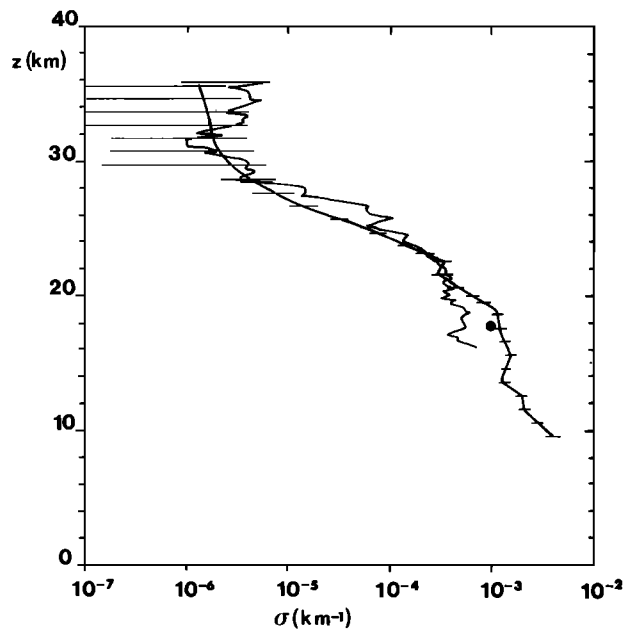


Fig. 12. Same as Figure 10, except $\lambda = 0.84 \mu\text{m}$. SAGE II data are converted from 1.02 to 0.84 μm with LND aerosol models, $v_{\text{eff}} = 0.25$; $r_{\text{eff}} = 0.35 \mu\text{m}$, $z < 22 \text{ km}$; $r_{\text{eff}} = 0.10 \mu\text{m}$, $z > 22 \text{ km}$. Solid circle is from balloon extinction.

height of 20 km was very close to the SAGE II tangent point [Ackerman *et al.*, 1987]. Figure 10 compares the balloon and the SAGE II extinction profiles at 0.375 and 0.385 μm , respectively; Figure 11 gives the same comparison for 0.440 and 0.453 μm ; the error due to the small difference in wavelength is in both cases smaller than 5%, and we have not found necessary to introduce a correction. Figure 12 presents the comparison of the balloon and the SAGE II extinction profiles at 0.84 μm . The SAGE II profile at 1.02 μm has been converted to 0.84 μm , using a LND model ($v_{\text{eff}} = 0.25$) with an effective radius of 0.10 μm above 22 km and 0.35 μm below 22 km, i.e., the model which gives the best agreement between lidar and SAGE II profiles (section 2, Figure 6); however, the conversion between 1.02 and 0.84 μm is not very sensitive to the choice of the model, as mentioned above. The balloon profiles exhibit oscillations which are smoothed on the SAGE II profiles. Above 21 km the general agreement is very good up to 26–28 km for the 0.44/0.453- μm and the 0.375/0.385- μm profiles, and up to 32 km for the 0.84- μm profile. Below 20 km the balloon profiles deduced from scattering could be of poorer quality. However, in this case the photographically measured extinction becomes significant and hence reliable. The value of aerosol extinction (total extinction minus Rayleigh and O₃ extinction) deduced from the balloon data agrees well with SAGE II results at 18 km altitude (Figure 12). Above 26 km the error bars on SAGE II profiles become very large for the short-wavelength channels and the oscillations of the balloon profiles increase toward high altitudes and short wavelengths. However, the balloon extinctions for 0.44 μm and 0.375 μm are systematically higher than the SAGE II extinctions above 26 km, which would point to smaller particles observed by the balloon.

The balloon limb photographs on April 22, 1985, provide an almost direct comparison with SAGE II profiles, for a close coincidence, and in a stable situation. The agreement

for the three wavelengths is very good between 21 and 26 km.

4. BALLOON POLARIMETRIC OBSERVATIONS

The instrument [Herman *et al.*, 1986] is a narrow field of view polarimeter operating at two wavelengths in the near-infrared, 0.85 and 1.65 μm . The scanning is performed in an horizontal plane by rotation of the gondola. Measurements of the radiance L and of the degree of polarization P at the two wavelengths can be made during the ascent and the descent or at the ceiling level; the best conditions are sunset or sunrise, when the Sun is close to the horizon, allowing the scattering angle θ to vary between 0° and 180° . The data are first corrected for multiple scattering and for the reflection by the ground or by the clouds, in the case when the Sun is above the horizon; the radiance is more conveniently expressed as a reflectance $\rho = \pi L/E$, where E is the solar irradiance. The inversion procedure uses first the polarization $P(\theta_0)$ at 1.65 μm ($\theta_0 = 100^\circ$), assuming that the molecular contribution is negligible; this defines a family of LND size distributions (r_m versus s); the reflectance $\rho(\theta_0)$ are used to retrieve the tangent optical depths for the two wavelengths; finally, the polarization $P(\theta_0)$ at 0.85 μm is used to select a model amongst the family found previously. It is checked that the reflectance $\rho(\theta)$ and polarization $P(\theta)$ computed with this model agree with the measured values for the two wavelengths and all the scattering angles.

Four flights took place, one for each period during the SAGE II European correlative program. All of the flights were launched from the Centre National d'Etudes Spatiales (CNES) Center at Aire sur l'Adour in the southwest of France. The four flights are briefly described here, and the results will be presented in section 5.2.

4.1. November 10, 1984

On November 10, 1984 (sunset flight) the aerosol layer was very inhomogeneous and unstable around the balloon. The data recorded between 14 and 30 km, with a gap due to transmission problems between 19 and 23 km, are therefore of poor quality. The polarization diagrams can be inverted only around 16–19 km.

4.2. November 28, 1984

On November 28, 1984 (sunrise flight) the conditions were better. Unfortunately, the balloon did not fly above 24 km, but good quality data were recorded between 14 and 24 km.

4.3. April 22, 1985

During the flight of April 22, 1985 (sunset), the instrument broke down at ceiling level. Data were recorded only during the ascent between 15 and 22 km and 27 and 30 km, when the gondola was not very stable and the Sun was still rather high above the horizon.

4.4. October 12, 1985

The flight of October 12, 1985, took place during sunset in good stable conditions, and data were recorded from 16 to 33 km. However, above 22 km the aerosol content was low, and the results are of better quality at low altitudes.

5. ANALYSIS OF THE RESULTS: VALIDATION OF THE THREE SHORT WAVELENGTH CHANNELS

The aerosol extinction coefficient is retrieved from SAGE II data at four wavelengths 1.02, 0.525, 0.453, and 0.385 μm ,

leading to a spectral extinction curve $\sigma^{\text{aer}}(\lambda)$ which could "in principle" be inverted to give the size distribution $n(r)$. The lidar backscattering profiles have been converted into extinction profiles at 1.02 μm using the aerosol model with $v_{\text{eff}} = 0.25$, which gives the best agreement with SAGE II profiles. Of course, varying v_{eff} , within a reasonable range, leads to a family of size distributions characterized by $(v_{\text{eff}}, r_{\text{eff}})$, which give the same conversion factor from lidar into extinction profiles. The model used for lidar conversion must be consistent with the model fitting the SAGE II spectral extinction $\sigma^{\text{aer}}(\lambda)$. The balloon polarization measurements lead to a retrieval of the size distribution $n(r)$, which best fit the polarization and the reflectance diagrams at 0.85 and 1.65 μm . This has also to be consistent with the SAGE II spectral extinction and with the lidar conversion factor. Finally, the balloon limb photographs provide profiles to be compared to the SAGE II short-wavelength extinction profiles (see Figures 8, 10, and 11).

Inverting the SAGE II spectral extinction $\sigma^{\text{aer}}(\lambda)$ is a rather delicate problem, and various approaches have been tried in order to retrieve two parameters of the size distribution, i.e., the effective radius r_{eff} and the effective variance v_{eff} , or the mean radius r_m and the variance s . The discussion of this inversion problem is beyond the scope of the present work and will be left for a future contribution. We limit ourselves here to deducing the effective radius r_{eff} [Lenoble and Brogniez, 1985] for an arbitrary fixed variance ($v_{\text{eff}} = 0.25$) from the ratio $\sigma^{\text{aer}}(0.453)/\sigma^{\text{aer}}(1.02)$, or more conveniently, from the related mean Angstrom coefficient α for the spectral interval 0.453/1.02 μm , defined by

$$\sigma^{\text{aer}}(\lambda) = \sigma^{\text{aer}}(1.02)\lambda^{-\alpha} \quad (12)$$

Preliminary tests with a two-parameter retrieval procedure suggest that the effective variance is generally smaller than 0.25 at the low levels below 22 km [Brogniez and Lenoble, 1989].

5.1. Consistency of Lidar Conversion Factor With SAGE II Spectral Extinction

November 10–13, 1984. For this period a stable situation is found only on November 13, when a lidar comparison was possible (Figure 2). If we look at the Angström coefficient α for the wavelength interval (0.453/1.02 μm) from the SAGE II profiles on November 13, it varies approximately from 0.6 to 1.8 when the altitude increases from 15 to 25 km, pointing to a decrease of the particle effective radius from about 0.40 to 0.20 μm with altitude; the variation of $\sigma^{\text{aer}}(\lambda)$ between 0.525 and 0.385 μm suggests, at least for the low altitudes, a rather small effective variance, around 0.1 or a little larger than 0.1. As mentioned earlier, the conversion factor from lidar backscattering into extinction is not very sensitive to the model for particles with r_{eff} larger than 0.20 μm , and the agreement found between the lidar and the SAGE II profiles in Figure 2 would remain had we used the aerosol models derived from the SAGE II spectral extinction instead of the model $r_{\text{eff}} = 0.35 \mu\text{m}$, $v_{\text{eff}} = 0.25$.

November 26–30, 1984. For this period the comparison between SAGE II and lidar profiles on November 27 (Figure 3) requires an aerosol model with $r_{\text{eff}} = 0.25 \mu\text{m}$ for $z < 21$ km, $r_{\text{eff}} = 0.10 \mu\text{m}$ for $21 \text{ km} < z < 26 \text{ km}$, and $r_{\text{eff}} = 0.05 \mu\text{m}$ for $z > 26 \text{ km}$. For the low altitudes, the SAGE II spectral extinction suggests r_{eff} between 0.35 and 0.24 μm (α between

0.8 and 1.5), which is consistent with the model ($r_{\text{eff}} = 0.25 \mu\text{m}$) chosen for the lidar conversion, considering the small sensitivity of the conversion factor in this size range. However, at higher altitudes, α increases from about 1.3 to 1.9, which means a decrease of r_{eff} from about 0.25 to 0.18 μm . Small particles, as chosen for the lidar conversion factor, would give α around 3; this is absolutely inconsistent with the SAGE II extinction values in the short-wavelength channels, which are much too low.

On November 28, as mentioned previously, the two SAGE II profiles are different above 25 km but quite close between 16 and 25 km, with a small extinction peak around 21 km for the western profile that does not appear on the eastern profile (Figure 4); in the peak the particles are slightly larger ($\alpha \approx 1.2$ for the western profile, instead of 1.4 at the same level in the eastern profile). The two lidar profiles (Frascati and OHP) are rather different, and the OHP profile agrees better with the SAGE II profiles. From SAGE II extinction profiles, α increases from 0.65 to 1.8 between 14 and 24 km, which means r_{eff} decreasing from 0.40 to 0.20 μm ; this is again consistent with the choice $r_{\text{eff}} = 0.35 \mu\text{m}$ for the lidar conversion factor.

On November 30 (Figure 5) we have the closest coincidence between a lidar and a SAGE II observation. The conversion factor for an aerosol model with $r_{\text{eff}} = 0.35 \mu\text{m}$ gives a very good agreement between 13 and 22 km (upper limit of the lidar profile). In this altitude range the SAGE II Angström coefficient varies from 0.6 to 1.4, which corresponds to particles with r_{eff} decreasing slightly from about 0.40 to 0.25 μm . This is again perfectly consistent with the choice of $r_{\text{eff}} = 0.35 \mu\text{m}$ for the conversion of lidar data.

April 1985. In April 1985 the aerosol layer over Europe during the observation period was very homogeneous and stable. The comparison between the SAGE II average profile and the Garmisch-Partenkirchen profile on April 21 was made using for the conversion factor $r_{\text{eff}} = 0.35 \mu\text{m}$ below 22 km and $r_{\text{eff}} = 0.10 \mu\text{m}$ above that level. The SAGE II spectral extinction gives r_{eff} decreasing from about 0.35 μm at 13 km, to 0.25 μm at 22 km, and then to 0.17 μm at 30 km ($\alpha \approx 0.9$, $\alpha \approx 1.4$, and $\alpha \approx 2.0$, respectively). This is consistent with the choice $r_{\text{eff}} = 0.35 \mu\text{m}$ for the lidar conversion factor below 22 km, but not at higher altitudes, where the SAGE II spectral extinction leads to particles much larger than the particles which are found necessary in order to obtain a good agreement between the lidar and the SAGE II profile. Again, we find the same difficulty as on November 27: the aerosol model derived from SAGE II spectral extinction would lead to a poor agreement with the lidar profile at high altitudes, whereas agreement is obtained by assuming much smaller particles than those given by SAGE II short-wavelength channels. The balloon limb photographs (section 3) on April 22 give extinction coefficients larger than SAGE II above 25 km for the short wavelengths (Figure 10 and 11), pointing to particles smaller than those retrieved from SAGE II. But it is difficult with the rapid oscillations of the balloon profiles to deduce the spectral variation $\sigma^{\text{aer}}(\lambda)$ at a given level and to make a quantitative comparison with SAGE II size distribution.

October 12, 1985. On this day the comparison between the SAGE II profile and the OHP lidar was made with $r_{\text{eff}} = 0.17 \mu\text{m}$, between 16 and 25 km, whereas the SAGE II spectral extinction leads to r_{eff} decreasing from 0.34 to 0.21 μm with altitude (α between 0.9 and 1.7). It is the only case

TABLE 1. Comparison of Aerosol Effective Radius r_{eff} Used for Lidar/SAGE II Best Fit at 1.02 μm and Retrieved From SAGE II Extinction Ratio $\sigma^{\text{aer}}(0.45)/\sigma^{\text{aer}}(1.02)$

Date	Altitude, km	r_{eff} (lidar), μm	r_{eff} (SAGE II), μm
November 13, 1984	12–25	0.35	0.40–0.20
November 27, 1984	12–21	0.25	0.35–0.24
	21–26	0.10	0.24–0.18
	26–30	0.05	0.18
November 28, 1984	12–23	0.35	0.40–0.20
November 30, 1984	13–32	0.35	0.40–0.25
April 21, 1985	10–22	0.35	0.35–0.25
	22–30	0.10	0.25–0.17
October 12, 1985	16–25	0.17	0.34–0.21

where we find some inconsistency between the best choice for the lidar conversion factor and the best fit to $\sigma^{\text{aer}}(\lambda)$ at low altitudes. In Figure 7 we have also drawn the extinction profile deduced from the lidar profile using the aerosol model, which fits both the polarization measurements (see discussion in section 5.2) and the SAGE II spectral extinction. The agreement with the SAGE II profile is definitely not as good as that obtained with the model $v_{\text{eff}} = 0.25$, $r_{\text{eff}} = 0.17 \mu\text{m}$, but the disagreement appears only below 20 km and remains rather small: it might be attributed to small local or temporal variation of the aerosol, as the observations are not exactly coincident either in location, or in time. These results are summarized in Table 1.

5.2. Balloon Polarimetric Observations and Size Distribution

The balloon polarimetric observations provide radiance and polarization diagrams at 0.85 and 1.65 μm , and their inversion leads to the retrieval of two parameters of the size distribution, assumed to be lognormal. However, it must be kept in mind that the actual aerosol size distribution may not be close to lognormal and may not even be monomodal. The retrieved size distribution must be understood as one of the many size distributions which give a good fit to the radiance and to the polarization of the diffuse radiation in the near-infrared. The inversion of the SAGE II spectral extinction between 0.385 and 1.02 μm is subject to the same remark as the inversion of the polarimetric data; the retrieved size distribution is one of many which give a good fit to the extinction coefficient in the visible range. Therefore using the balloon polarimetric data to validate the SAGE II short-wavelength channels is a rather delicate task, and the results must be considered with caution.

November 10, 1984. For the flight of November 10, 1984, Figure 13 compares the tangent optical depth at 1.02 μm observed from SAGE II on November 10 and 11 with the tangent optical depth observed by the balloon instrument. As noted previously, the SAGE II event tangent point is closer to the balloon launch site on November 11 than on November 10. The balloon data exhibit strong oscillations and have been averaged over 1 km. The balloon optical depth values at 0.85 μm have been converted into values at 1.02 μm , using an aerosol effective radius of 0.28 μm below 20 km and of 0.10 μm above 22 km; the influence of the model choice is, however, small. The balloon tangent optical depth profile given by the polarimeter is closer to the SAGE II profile on November 10, whereas the extinction profile

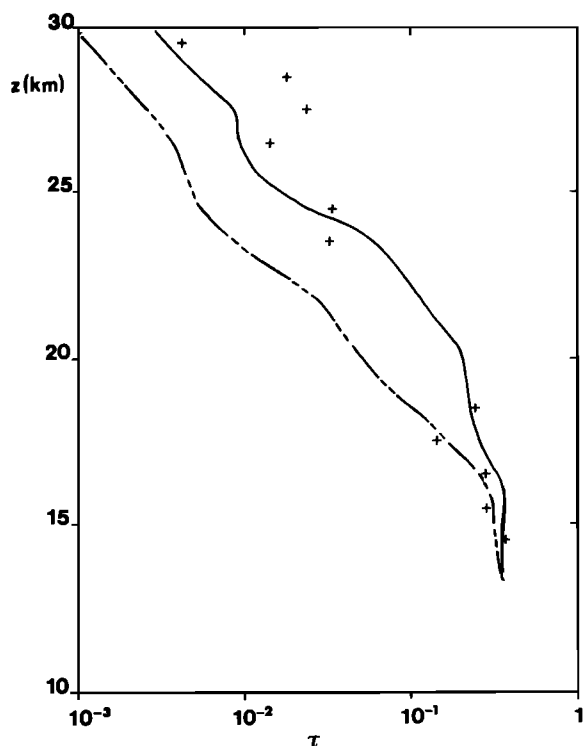


Fig. 13. Comparison of the tangent optical depth at $1.02 \mu\text{m}$, measured by SAGE II on November 10, 1984, at 1627 UT, 37.80°N , 5.27°E (solid curve) and on November 11, 1984, 1639 UT, 40.50°N , 56°E (dash-double-dotted curve), and measured by the balloon polarimeter on November 10, 1984, sunset, launch site 44°N , 0° (crosses). The conversion of the balloon data from 0.85 to $1.02 \mu\text{m}$ has been done with $r_{\text{eff}} = 0.28 \mu\text{m}$ below 20 km and $r_{\text{eff}} = 0.10 \mu\text{m}$ above 22 km.

deduced from the balloon limb photographs on the same day was closer to the SAGE II profile on November 11. This is not too surprising in a very unstable situation, as the two balloons were not operating exactly at the same place and at the same time. The complete inversion of the polarization data has been performed only for the altitude range 16 – 19.5 km; the retrieved size distribution has an effective radius $r_{\text{eff}} \approx 0.35 \mu\text{m}$ and an effective variance $v_{\text{eff}} \approx 0.17$ between 16 and 17 km; between 17.5 and 19.5 km the effective radius is slightly smaller; $r_{\text{eff}} \approx 0.29 \mu\text{m}$ with $v_{\text{eff}} \approx 0.14$. This is in excellent agreement with the size distribution retrieved from the SAGE II extinction ratio $\sigma^{\text{acr}}(0.45)/\sigma^{\text{acr}}(1.02)$, which gives, for November 11, r_{eff} decreasing from 0.32 to $0.23 \mu\text{m}$, if we assume $v_{\text{eff}} = 0.25$, and from 0.36 to $0.27 \mu\text{m}$ for $v_{\text{eff}} = 0.10$, between 15 and 20 km. For November 10, SAGE II data give, for the same altitude range of 15 – 20 km, an almost constant effective radius $r_{\text{eff}} = 0.30 \mu\text{m}$, if we assume $v_{\text{eff}} = 0.25$, and $r_{\text{eff}} = 0.33 \mu\text{m}$ with $v_{\text{eff}} = 0.10$.

November 28, 1984. This flight took place in more stable conditions. The tangent optical depth measured by the balloon above 20 km is larger, by about a factor of 2, than the optical depth measured by SAGE II, whereas at the lower levels (13 – 17 km) the two values agree reasonably well. No explanation has been found for this disagreement, which may just be due to local conditions. The polarization data lead to a size distribution with an effective radius that is almost constant around $0.22 \mu\text{m}$, and an effective variance decreasing from 0.80 to 0.18 between 15 and 22 km. The SAGE II extinction ratio $\sigma^{\text{acr}}(0.45)/\sigma^{\text{acr}}(1.02)$ leads to an

effective radius decreasing from 0.38 to $0.22 \mu\text{m}$, assuming $v_{\text{eff}} = 0.25$, for the same altitude range. The large variance found by the balloon at low levels seems to confirm the presence of particles different from those observed by SAGE II.

April 22, 1985. Unfortunately, on April 22, 1985, no inversion of the polarization diagram was possible owing to the instability of the data. However, at a few levels a relative stabilization appeared, and the diagram can be used for direct comparisons. Figure 14 shows the polarization diagram for the two wavelengths (0.85 and $1.65 \mu\text{m}$) and three altitude levels (15 , 18.2 , and 21.5 km); the dots are the experimental data and present a rather large dispersion. The solid lines show the polarization computed with models derived from a best fit to the SAGE II spectral extinction ($v_{\text{eff}} = 0.17$; $r_{\text{eff}} = 0.37 \mu\text{m}$ at 15 km, and $r_{\text{eff}} = 0.29 \mu\text{m}$ at 18.2 km and 21.5 km). The comparison is satisfying. Unfortunately, no such comparison was possible at higher levels.

October 12, 1985. The flight of October 12, 1985, provides another good comparison to SAGE II data. Figure 15 presents the vertical profiles of r_{eff} and v_{eff} retrieved from the polarization data. Above 22 km the effective variance increases rapidly and stabilizes around 0.9 , whereas the effective radius presents very large oscillations; these results at high altitudes are certainly dubious, because the aerosol content becomes very low above 22 km and the signal-to-noise ratio becomes bad. However, the large value retrieved for v_{eff} could suggest that the size distribution becomes bimodal at high altitudes; therefore the retrieval procedure, which assumes a monomodal distribution, leads to erratic results. Figure 16 demonstrates, for 17.5 km, the good quality of the inversion. Figure 17 shows the tangent optical depth at $1.02 \mu\text{m}$ deduced from the measured optical depth at $0.85 \mu\text{m}$, using LND models which incorporate, at each altitude, the effective radius and the effective variance retrieved from the polarization data and averaged over 1 km; it is compared with the SAGE II tangent optical depth at $1.02 \mu\text{m}$ on the morning of October 12, 1985, 7° west of the launch site. The similarity above 16 km between the four SAGE II profiles over the zone on October 12 and 13 justify the comparison, despite the not very close coincidence in time and location. Figure 18 compares the extinction ratios for the three short wavelengths $\sigma^{\text{acr}}(0.525)/\sigma^{\text{acr}}(1.02)$, $\sigma^{\text{acr}}(0.45)/\sigma^{\text{acr}}(1.02)$, $\sigma^{\text{acr}}(0.385)/\sigma^{\text{acr}}(1.02)$ measured by SAGE II and computed at each level with the size distribution retrieved from the polarization data and averaged over 1 km. As a result of the low aerosol content, the extinction ratios derived from the polarization data are somewhat inaccurate. However, the agreement is good.

6. CONCLUSIONS

Although the SAGE II $1.02\text{-}\mu\text{m}$ channel allows retrieval of the extinction profile at very low levels, only the profiles a few kilometers above the tropopause (12 – 15 km) and higher have been considered; at lower altitudes the variability is such that only almost coincident observations would be necessary to validate SAGE II profiles.

From the data and the discussions presented in the previous sections, we must consider separately two altitude ranges. For safety, we will refer them as below 23 km and above 25 km, it being understood that the cutoff between the two ranges is somewhat variable, depending on the events and on the kind of observations.

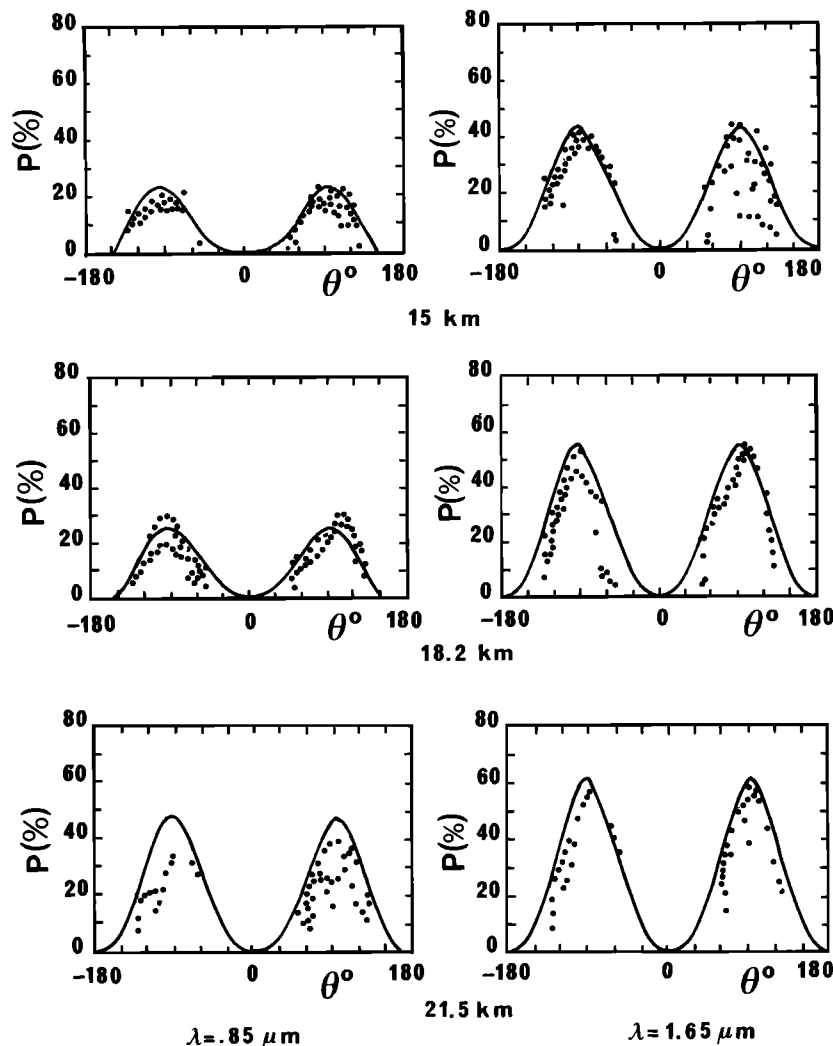


Fig. 14. Comparison on April 22, 1985, between the degree of polarization measured by the balloon polarimeter (dots) and computed using an aerosol model that fits the SAGE II spectral extinction (solid curve). The degree of polarization is given in percent versus the scattering angle. The left side curves are for $0.85 \mu\text{m}$ and the right side curves for $1.65 \mu\text{m}$; the top panel is at 15 km, the middle panel at 18.2 km, and the bottom panel at 21.5 km.

6.1. Altitude Range Below 23 km

Below 23 km, we have at our disposal a large series of data, including lidar profiles (both ruby and Nd: Yag), limb photographs, and polarization diagrams. The main conclusions are as follows:

1. The SAGE II extinction profiles at $1.02 \mu\text{m}$ agree within the error bars with the several extinction profiles deduced from the lidar backscattering profiles using a conversion factor, consistent with the SAGE II spectral variation of the extinction coefficient (Figures 2–7 and Table 1). These comparisons comprise one case (November 30, 1984) of very close coincidence in time (4 hours) and in location (100 km) between the lidar and the SAGE II observations, and several cases with a very stable and homogeneous aerosol layer, as proved by the comparisons between various SAGE II and lidar profiles over Europe for the experiment period. However, the consistency of the chosen backscatter into extinction conversion factor with the aerosol size distribution, retrieved from the four-wavelength SAGE II extinction, does not really validate the SAGE II four channels because the conversion factor is almost insensitive

to the aerosol model as long as the effective radius is larger than $0.20 \mu\text{m}$, which is the case in this altitude range.

2. The SAGE II extinction profile at $1.02 \mu\text{m}$ also agrees with the limb photographs profile at $0.84 \mu\text{m}$, the conversion between 1.02 and $0.84 \mu\text{m}$ being only very slightly sensitive to the aerosol model; the agreement is particularly good on April 22, 1985 (Figure 12) when the conditions are quite stable and the coincidence very close.

3. The SAGE II tangent optical depth profiles at $1.02 \mu\text{m}$ generally agree within the error bars with the optical depth profiles obtained by the balloon-borne polarimetric instrument.

4. The SAGE II extinction profiles at 0.453 and $0.385 \mu\text{m}$ have been compared directly to the extinction profiles at about the same wavelengths deduced from the limb photographs. April 22, 1985 (Figures 10 and 11) corresponds to a close coincidence (sunset, less than 100 km between the two observations). Despite the oscillations revealed by the high resolution of the photographs, the general agreement between the balloon and the SAGE II profiles is a good validation of the two channels 0.453 and $0.385 \mu\text{m}$, for the altitude range 21–25 km.

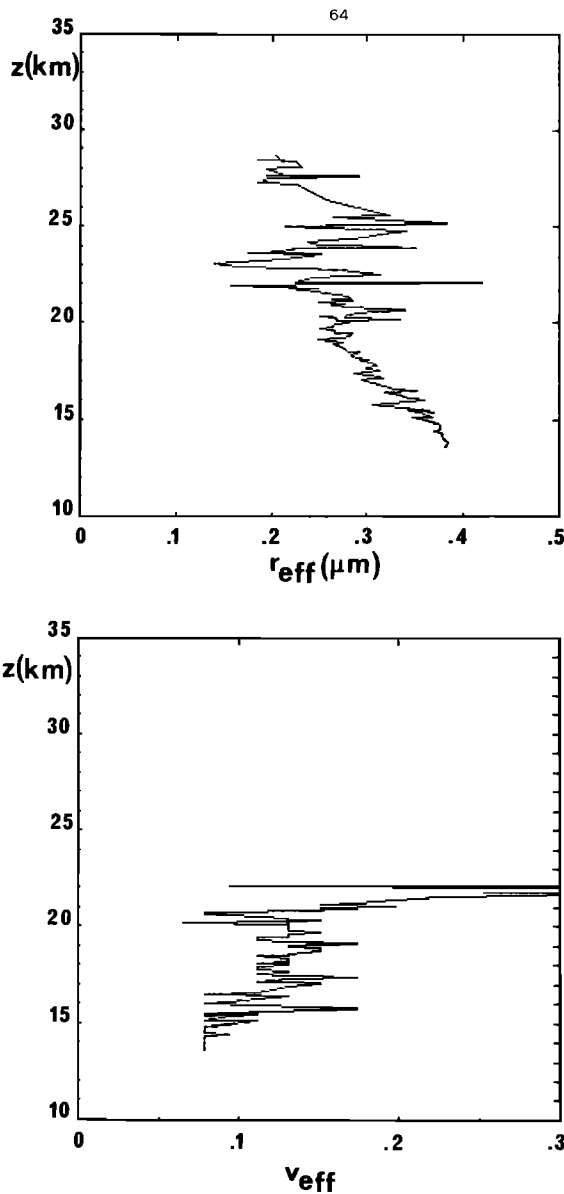


Fig. 15. (Top) Vertical profiles of the effective radius and (bottom) of the effective variance of the aerosol size distribution retrieved from the balloon polarimetric data on October 12, 1985.

5. The size distributions derived from the balloon polarization measurements and from SAGE II spectral extinction generally agree; the extinction ratio profiles $\sigma^{\text{acr}}(\lambda)/\sigma^{\text{acr}}(1.02)$ at 0.525, 0.453, and 0.385 μm , computed with the size distribution retrieved from the polarization measurements on October 12, 1985, agree well within the error bars with the corresponding SAGE II profiles (Figure 18). This is again a satisfying validation of the SAGE II short wavelength channels.

6.2. Altitude Range Above 25 km

Above 25 km, the situation is not as good. Most instruments failed in observing the low content of aerosols at these altitudes, and only a few data remain available: ruby lidar profiles on November 27, 1984, and April 21, 1985, and limb photograph profiles on April 22, 1985. Even these available data are not of the same quality as at lower levels. On the other hand, whereas the SAGE II profile at 1.02 μm remains

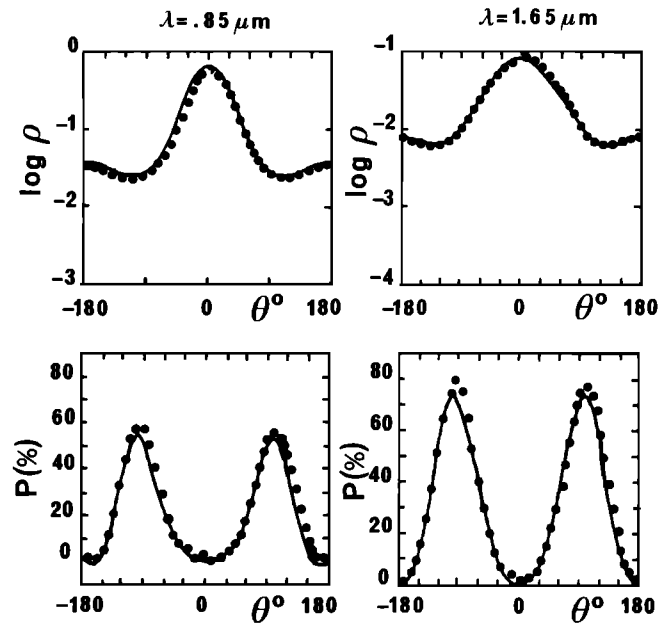


Fig. 16. Test of the inversion of the balloon polarimetric data on October 12, 1985. The dots are the measured values, which are to be compared with the curves computed with the retrieved aerosol model. (Top) Reflectance at 0.85 μm (left) and 1.65 μm (right). (Bottom) Degree of polarization in percent at 0.85 μm (left) and 1.65 μm (right) versus the scattering angle.

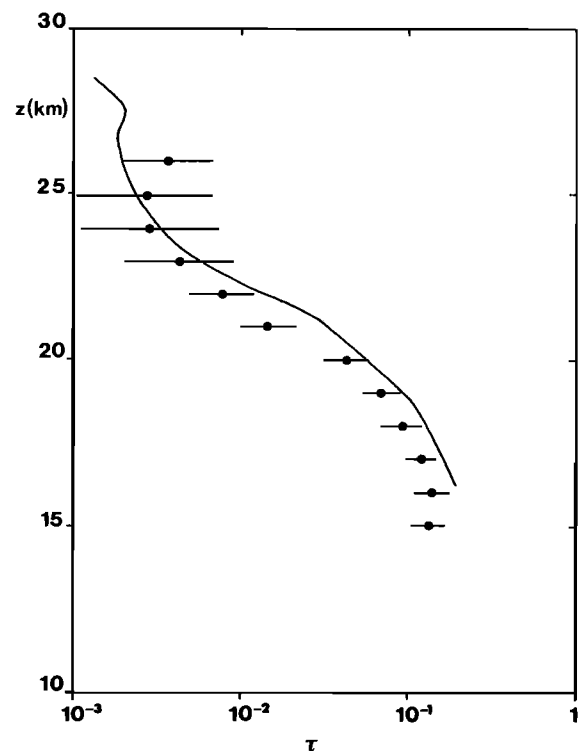


Fig. 17. Comparison of the tangent optical depth at 1.02 μm , measured by SAGE II on October 12, 1985, at 0639 UT, 41.25°N, -7.10°E (solid curve) and by the balloon polarimeter on October 12, 1985, at sunset, launch site 44°N, 0° (solid circles). The conversion of the balloon data from 0.85 to 1.02 μm has been made with the aerosol model retrieved from the polarization data.

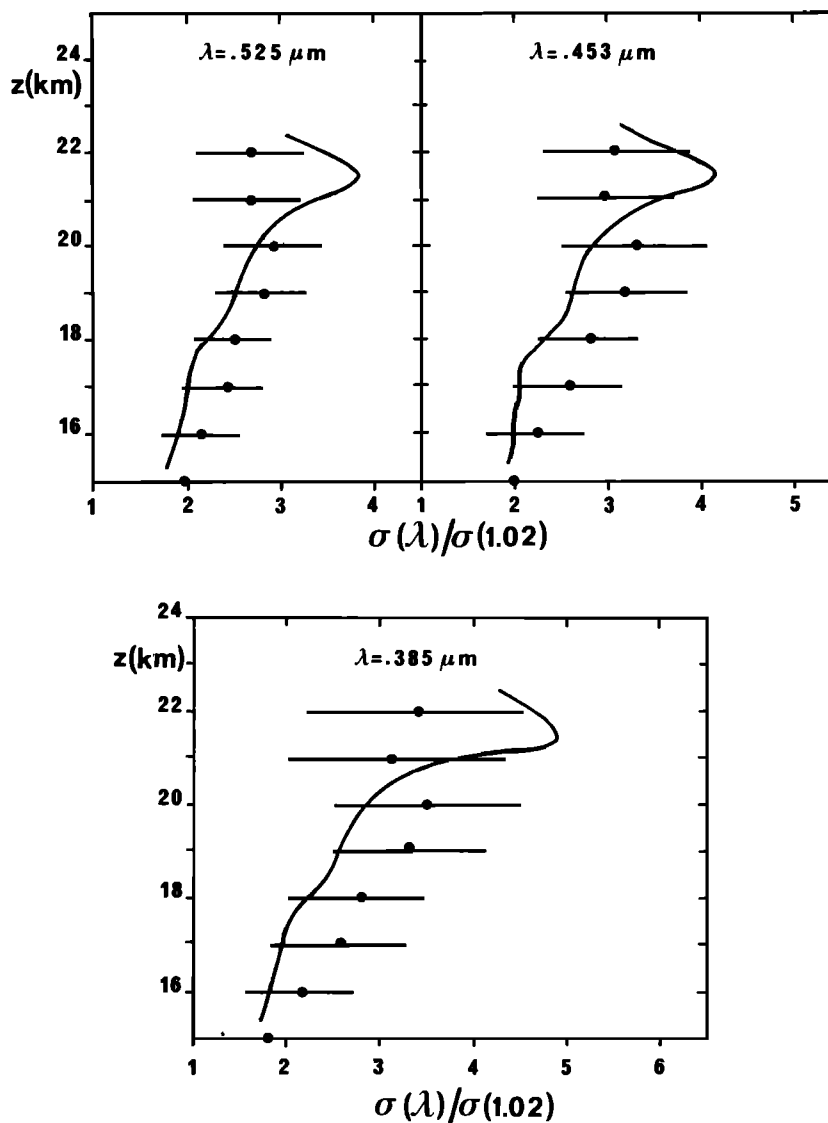


Fig. 18. Comparison of the aerosol extinction ratio $\sigma^{acr}(\lambda)/\sigma^{acr}(1.02)$ measured by SAGE II on October 12, 1985, at 0639 UT, 41.25°N, 7.10°E (solid curve) and computed using the aerosol model retrieved from the balloon polarization data on October 12, 1985, at sunset, launch site 44°N, 0° (solid circles); (Top) Curve on left, $\lambda = 0.525 \mu\text{m}$, curve on right, $\lambda = 0.453 \mu\text{m}$. (Bottom) curve shows $\lambda = 0.385 \mu\text{m}$.

rather good up to 30 km, the three short-wavelength profiles have increasingly large error bars above 25 km. The main conclusions for the high altitude range are the following:

1. The extinction profiles at 1.02 μm deduced from the lidar backscattering profiles can be put into agreement with the SAGE II profiles (Figures 3 and 6), using for the conversion of backscattering into extinction an aerosol model with very small particles ($r_{\text{eff}} \approx 0.10 \mu\text{m}$ to $0.05 \mu\text{m}$). This choice is inconsistent with the size distribution derived from the SAGE II spectral variation of extinction, which leads to $r_{\text{eff}} \approx 0.18 \mu\text{m}$. In this size range the conversion factor of backscattering into extinction is very sensitive to the aerosol model, and choosing $r_{\text{eff}} = 0.18 \mu\text{m}$ would destroy the agreement of the SAGE II and the lidar profiles in Figures 3 and 6.

2. The limb photography profile at 0.84 μm agrees perfectly well (Figure 12) with the 1.02- μm SAGE II profile converted at 0.84 μm (conversion not very sensitive to the model choice).

3. The limb photography profiles at the short wavelengths show extinction significantly larger than SAGE II (Figures 10 and 11). This suggests particles with r_{eff} smaller than 0.18 μm , but the very large oscillations of the profiles do not allow a retrieval of r_{eff} .

Whereas a good validation of SAGE II aerosol extinction profiles is obtained below 23 km, it seems difficult to draw a clear conclusion from the few observations above 25 km. It is likely that the SAGE II 1.02- μm profile, which has small error bars, remains good. But the three SAGE II short-wavelength channels, as well as the ruby lidar profile and the limb photographs, have very large uncertainties at these high levels; it is hard to decide what must be better believed.

A very tentative guess to explain at least a part of the contradiction at high altitudes is that the size distribution becomes bimodal; for a fixed value of the ratio $\sigma^{acr}(0.45)/\sigma^{acr}(1.02)$, it has been shown [Lenoble and Brogniez, 1985] that the lidar conversion factor generally increases when a second mode is added to a size distribution. Qualitatively,

this could reconcile the SAGE II spectral extinction with the choice of the conversion factor necessary to have agreement between the lidar and the SAGE II 1.02- μm profile. This could also explain the bad quality of the polarization data inversion and the rapid increase of v_{eff} above 23 km.

Acknowledgments. The authors are grateful to the organizations that have provided financial support for their participation in this program. The success of the balloon flights is due to the efficient help of the staff of The CNES center at Aire sur l'Adour. The SAGE II data were kindly provided by the NASA Langley Research Center.

REFERENCES

- Ackerman, M., C. Lippens, and C. Muller, Stratospheric aerosol properties from Earth limb photography, *Nature*, **292**, 587–591, 1981.
- Ackerman, M., C. Lippens, and D. De Muer, Wave signature in stratospheric aerosols, *Geophys. Res. Lett.*, **12**, 445–447, 1985.
- Ackerman, M., W. Chu, C. Lippens, and D. De Muer, SAGE II aerosol extinction and scattering data from balloon borne photography, *Adv. Space Res.*, **7**, 243–249, 1987.
- Brogniez, C., and J. Lenoble, Size distribution of stratospheric aerosols from SAGE II multiwavelength extinction, in *Aerosols and Climate*, edited by P. V. Hobbs and M. P. McCormick, pp. 305–312, A. Deepak Publishing, Hampton, Va., 1989.
- Chu, W. P., M. P. McCormick, J. Lenoble, C. Brogniez, and P. Pruvost, SAGE II inversion algorithm, *J. Geophys. Res.*, this issue.
- Herman, M., J. Y. Balois, L. Gonzalez, P. Lecomte, J. Lenoble, R. Santer, and C. Verwaerde, Stratospheric aerosol observations from a balloon-borne polarimetric experiment, *Appl. Opt.*, **25**, 3573–3584, 1986.
- Hofmann, D. J., J. M. Rosen, R. Reiter, and H. Jäger, Lidar- and balloon-borne particle counter comparisons following recent volcanic eruptions, *J. Geophys. Res.*, **88**, 3777–3782, 1983.
- Lenoble, J., Presentation of the European correlative experiment program for SAGE II, *J. Geophys. Res.*, this issue.
- Lenoble, J., and C. Brogniez, A comparative review of radiation aerosol models, *Contrib. Atmos. Phys.*, **57**, 1–20, 1984.
- Lenoble, J., and C. Brogniez, Information on stratospheric aerosol characteristics contained in the SAGE satellite multiwavelength extinction measurements, *Appl. Opt.*, **24**, 1054–1063, 1985.
- Oberbeck, V. R., J. Livingston, R. Pueschel, K. Snetsinger, G. Ferry, W. Fong, and S. Verma, Aerosol sampling for the August 7th, and 9th, 1985 SAGE II validation experiment, paper presented at Sixth Conference on Atmospheric Radiation, Am. Meteorol. Soc., Williamsburg, Va., May 12–16, 1986.
- Osborn, M. T., J. N. Rosen, M. P. McCormick, P. Wang, J. M. Livingstone, and T. J. Swissler, SAGE II aerosol correlative observations: Profile measurements, *J. Geophys. Res.*, this issue.
- Russell, P. B., et al., Satellite and correlative measurements of the stratospheric aerosol, II, Comparison of measurements made by SAM II, dustsondes, and an airborne lidar, *J. Atmos. Sci.*, **38**, 1295–1312, 1981.
- Russell, P. B., M. P. McCormick, T. J. Swissler, J. M. Rosen, D. J. Hofmann, and L. R. McMaster, Satellite and correlative measurements of the stratospheric aerosol, III, Comparison of measurements by SAM II, SAGE, dustsondes, filters, impactors and lidar, *J. Atmos. Sci.*, **41**, 1791–1800, 1984.
- M. Ackerman and C. Lippens, Institut d'Aéronomie Spatiale de Belgique, 3 Avenue Circulaire, B1180 Brussels, Belgium.
- C. Brogniez, B. S. Diallo, M. Herman, J. Lenoble and R. Santer, Laboratoire d'Optique Atmosphérique, Université des Sciences et Techniques de Lille, 59655 Villeneuve d'Ascq cedex, France.
- G. Fiocco, Istituto di Fisica "Guglielmo Marconi," Università Degli Studi Roma, Piazzale Aldo Moro 2, I-00185 Rome, Italy.
- P. Gobbi, Istituto di Fisica dell'Atmosfera, Consiglio Nazionale delle Ricerche, CP 27, 00044 Frascati, Italy.
- M. Jäger, Institut für Atmosphärische Umweltforschung, Kreuzteckbahnstrasse 19, D 8100 Garmisch-Partenkirchen, Federal Republic of Germany.
- G. Megie and J. Pelon, Service d'Aéronomie du Centre National de la Recherche Scientifique, B.P. 3, 91371 Verrières-le-Buisson, France.
- R. Reiter, Consulting Bureau, Fritz Mullerstrasse 54, D 8100 Garmisch-Partenkirchen, Federal Republic of Germany.

(Received April 4, 1988;
revised February 3, 1989;
accepted February 3, 1989.)